Fast $E2$ Transitions*

A. W. SUNYAR
Brookhaven National Laboratory, Upton, New York
(Received January 11, 1955)

Lifetime measurements in the 10^{-9} sec range have been made for $E2$ or $M1+E2$ transitions in the following nuclei: Sm^{152}, Gd^{154}, Hf^{180}, W^{182}, Os^{188}, Ir^{191}, Au^{197}, and Po^{210}. Upper limits for lifetimes have been established for $E2$ or $M1+E2$ transitions in Ir^{191}, Pb^{204}, Pb^{206}, Pb^{207}, and U^{234}. $E2$ radiative transition probabilities are considered within the framework of the Bohr-Mottelson unified nuclear model. For neutron number $N=90-126$, distortion parameters evaluated from $E2$ radiative lifetimes are about 5–6 times smaller than those evaluated from first excited state energies of even-even nuclei.

I. INTRODUCTION

SOME electric quadrupole transitions between nuclear states were known to exhibit radiative lifetimes much shorter[1] than those indicated by the lifetime estimates made on the basis of single-particle models.[2,3] The existence of such fast $E2$ transitions in the rare-earth region suggested that these were transitions of a "cooperative" type.[1] In the same region of the periodic table, the collective behavior of nuclear constituents appears in a number of additional ways (e.g., large static quadrupole moments of nuclear ground states in the rare-earth region). These large quadrupole moments have been interpreted[4] as evidence for deformation of a nuclear core by a particle structure. The ease of excitation of the nuclear core in the rare-earth region is shown by the uniformly low ($\sim$100 kev or less) and smoothly varying energies of first excited states[5,6] of even-even nuclei. The increasing energy of first excited states as magic numbers are approached illustrates the increasing core stability as major nucleon shells close.

In the nuclear model of Bohr and Mottelson,[7] individual particle and collective aspects of nuclear motion are combined. The existence of an equilibrium deformation of the nucleus allows rotational motion of the system as a whole, leading to a rotational spectrum for even-even nuclei with spin states $I=0+$, $2+$, $4+$, $\cdots$ and energies proportional to $I(I+1)$. $E2$ radiative transitions between such rotational states are much enhanced through the large quadrupole moment of the deformed core. Within the framework of the model, a measure of the nuclear deformation is provided by the $E2$ radiative transition probabilities between rotational states.

Since core deformation is known to correlate with shell structure, particularly in the behavior of quadrupole moments[8] and first excited state energies,[5,6] it is of interest to correlate γ-transition matrix elements for $E2$ transitions in a similar way. Since the core becomes increasingly stable against deformation as major particle shells close, we may qualitatively expect that $E2$ γ-transition matrix elements between rotational states achieve a maximum value in the rare-earth region where core deformations are large, and decrease more or less regularly as magic numbers are approached.

Empirical information about the radiative properties of $E2$ transitions has been somewhat limited. We have accordingly attempted to measure the lifetimes of a number of additional $E2$ transitions in even-even nuclei.

II. EXPERIMENTAL ARRANGEMENT

The lifetime measurements were made by fast coincidence techniques, using a delayed-coincidence scintillation spectrometer of short resolving time $2\tau\simeq 3\times 10^{-9}$ sec. The coincidence system is shown in block diagram in Fig. 1. The detectors used in these measurements were *trans*-stilbene phosphors, mounted on RCA 5819 photomultipliers. For detection of soft conversion electrons the source was usually mounted directly on a thin ($\sim$0.5 mm) *trans*-stilbene phosphor. The photomultipliers were operated at 1200 to 1400 volts. The photomultiplier pulses were amplified by one Hewlett-Packard wide-band amplifier. The fast-coincidence arrangement is similar to those previously described.[9–11]

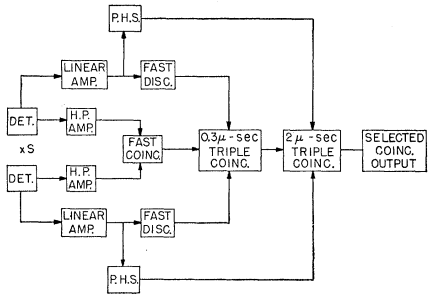

FIG. 1. Block diagram of fast-coincidence system.

* Under the auspices of the U. S. Atomic Energy Commission.
[1] M. Goldhaber and A. W. Sunyar, Phys. Rev. **83**, 906 (1951).
[2] V. F. Weisskopf, Phys. Rev. **83**, 1073 (1951).
[3] S. A. Moszkowski, Phys. Rev. **83**, 1071 (1951).
[4] J. Rainwater, Phys. Rev. **79**, 432 (1950).
[5] G. Scharff-Goldhaber, Phys. Rev. **90**, 587 (1953).
[6] P. Preiswerk and P. Stähelin, Nuovo cimento **10**, 1219 (1953).
[7] A. Bohr and B. R. Mottelson, Kgl. Danske Videnskab. Selskab, Mat.-fys. Medd. **27**, No. 16 (1953).
[8] Townes, Foley, and Low, Phys. Rev. **76**, 1415 (1949); Kenneth W. Ford, Phys. Rev. **90**, 29 (1953).
[9] Bell, Graham, and Petch, Can. J. Phys. **30**, 35 (1952).
[10] F. K. McGowan, Oak Ridge National Laboratory Report, ORNL-952, 1951 (unpublished).
[11] S. de Benedetti and H. J. Richings, Rev. Sci. Instr. **23**, 37 (1952).

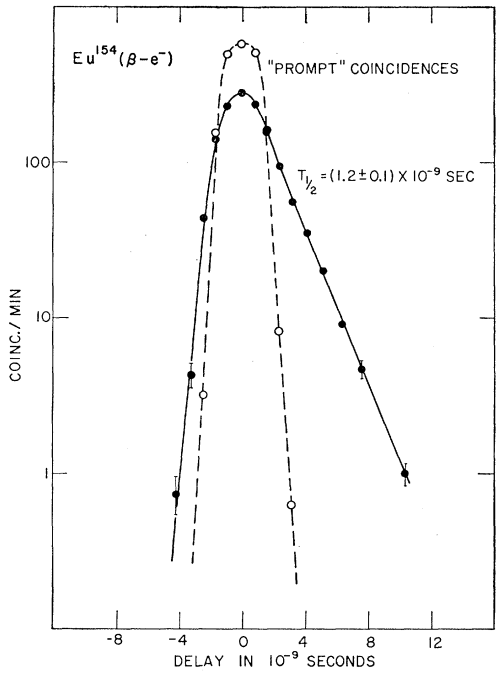

FIG. 2. Time distribution of coincidences between a portion of the β spectrum from Eu^{154} and conversion electrons of the 123-kev transition in Gd^{154}.

Pulse equalization was achieved by pentode limiters and the limited plate signals were shaped by a shorted delay line. The introduction of delays into either channel was achieved by inserting lengths of *RG* 7/*U* cable (4×10^{-9} sec/meter). Selection of coincidences was achieved by a suitably biased germanium diode

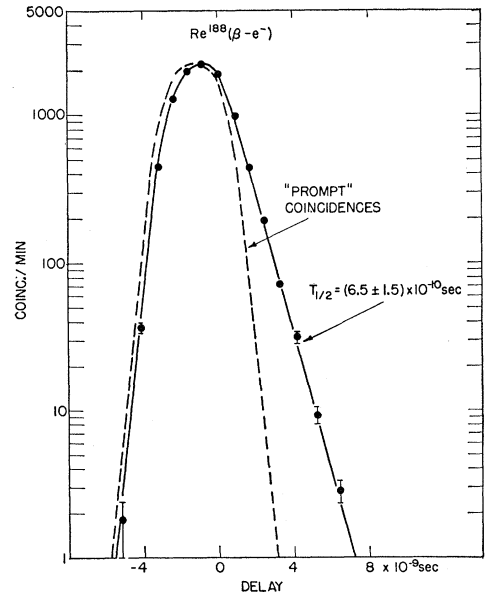

FIG. 3. Time distribution of coincidences between a portion of the β spectrum from Re^{188} and conversion electrons of the 155-kev transition in Os^{188}.

General Electric *G* 7-*A*). This unselected fast-coincidence output was mixed ($\tau\simeq0.3\times10^{-6}$ sec) with the output signals of two lower-edge integral discriminators operating on signals which originated from a late dynode of the photomultipliers. The output of this relatively slow coincidence circuit could be finally mixed ($\tau\approx2\times10^{-6}$ sec) with the outputs of two single-channel pulse height analyzers for pulse height selection.

The effects of variations in input pulse size on the resolution curve of a coincidence system have been previously discussed.[9] A measurement of a short nuclear lifetime by centroid analysis[12,13] of the resolution curve requires close control of input pulse size. Such control is normally imposed by narrow-window pulse-height selection on the pulses from both counters and necessarily reduces the coincidence counting rate by a large factor. It is often sufficient to impose only a lower limit on the amplitude of signals accepted. Such a procedure is satisfactory if the sides of the "prompt" resolution curve fall off sufficiently rapidly for the smallest accepted signals to allow "exponential tail" determinations of lifetimes. A particular lifetime measurement can be made considerably more rapidly with integral discrimination than with narrow-window pulse height selection, but it is clear that the ultimate performance of a coincidence system may be achieved only with the latter technique.

For the lifetime measurements reported here, it was usually but not always sufficient to impose only a lower limit on the amplitude of accepted signals. It was occasionally advantageous to employ integral discrimination in one channel and narrow-window pulse-height discrimination in the second channel to reject signals leading to coincidences not of immediate interest. Whenever necessary, any results obtained

TABLE I. Lifetimes for *E*2 transitions in even-even nuclei.

Nucleus	*E*(kev)	$T_{\frac{1}{2}}$(in 10^{-9} sec)
Sm^{152}	122	1.40±0.10
Gd^{154}	123	1.20±0.10
Hf^{180}	93	1.40±0.10
W^{182}	100	1.27±0.10
Os^{188}	155	0.65±0.15
Po^{210}	46.7	1.5 ±0.2
Pb^{204}	890	<0.6
Pb^{206}	803	<0.5
U^{234}	43.6	<0.5

TABLE II. Lifetimes for *E*2 transitions in odd-*A* nuclei.

Nucleus	*E*(kev)	$T_{\frac{1}{2}}$(in 10^{-9} sec)	Multipole character
Ir^{191}	82.3	3.85±0.35	*M*1+*E*2
Ir^{191}	129	<0.5	*M*1+*E*2
Au^{197}	77.4	1.90±0.20	*M*1+*E*2
Pb^{207}	570	<0.4	*E*2

[12] T. D. Newton, Phys. Rev. **78**, 490 (1950).
[13] Z. Bay, Phys. Rev. **77**, 419 (1950).

under conditions where only integral discrimination was imposed were checked with narrow-window pulse-height selection.

III. RESULTS AND DISCUSSION

Typical delayed coincidence curves are shown in Figs. 2 and 3. A summary of our new experimental results for even-even nuclei is presented in Table I. In addition, lifetimes or lifetime limits have been determined for the transitions in odd-A nuclei listed in Table II.

The available data concerning $E2$ transitions in even-even nuclei with neutron number $N=90-142$ (Sm to U) is summarized in Table III. The radiative mean life $\tau_\gamma = T_{\frac{1}{2}}(1+\alpha)/\ln 2$, where α is the total internal conversion coefficient and $T_{\frac{1}{2}}$ is the experimental half-life. In a few cases the conversion correction could be made by utilizing measured values of α_K and $K/(L+M)$ ratios where reliable data were available. It was usually necessary, however, to interpolate the L-shell compu-

TABLE III. Summary of $E2$ γ-ray lifetimes in even-even nuclei.

Nucleus	E(kev)	$T_{\frac{1}{2}}$(sec)	Estimated conversion	τ_γ(sec)	$I_i\pi_i \rightarrow I_f\pi_f$
$_{92}U^{234}$	43.6	$<5\times10^{-10}$	930	$<6.7\times10^{-7}$	$2+\rightarrow0+$
$_{88}Ra^{226}$	67.8	$<1.4\times10^{-9}$	75	$<1.5\times10^{-7}$	$2+\rightarrow0+$
$_{84}Po^{210}$	46.7	1.5×10^{-9}	300	6.5×10^{-7}	$(4,5,6+)\rightarrow4+$
$_{82}Pb^{208}$	583	2.4×10^{-10}	0.021	3.5×10^{-10}	$5-\rightarrow3-$
$_{82}Pb^{206}$	803	$<5\times10^{-10}$	~0.01	$<7.3\times10^{-10}$	$2+\rightarrow0+$
$_{82}Pb^{204}$	374	2.6×10^{-7}	0.06	4.0×10^{-7}	$(4+\rightarrow2+)$
$_{82}Pb^{204}$	890	$<6\times10^{-10}$	~0.01	$<10^{-9}$	$(2+\rightarrow0+)$
$_{80}Hg^{198}$	411	2.1×10^{-11}	0.04	3.15×10^{-11}	$2+\rightarrow0+$
$_{76}Os^{188}$	155	6.5×10^{-10}	0.95	1.83×10^{-9}	$2+\rightarrow0+$
$_{76}Os^{186}$	137	8.0×10^{-10}	1.4	2.77×10^{-9}	$2+\rightarrow0+$
$_{74}W^{182}$	100	1.27×10^{-9}	4.6	1.03×10^{-8}	$2+\rightarrow0+$
$_{72}Hf^{180}$	93	1.4×10^{-9}	5.6	1.32×10^{-8}	$2+\rightarrow0+$
$_{72}Hf^{176}$	89	1.35×10^{-9}	6.7	1.5×10^{-8}	$2+\rightarrow0+$
$_{70}Yb^{170}$	84.1	1.57×10^{-9}	7.4	1.91×10^{-8}	$2+\rightarrow0+$
$_{68}Er^{166}$	80.8	1.7×10^{-9}	8.1	2.23×10^{-8}	$2+\rightarrow0+$
$_{68}Er^{164}$	90.5	1.4×10^{-9}	5.6	1.33×10^{-8}	$2+\rightarrow0+$
$_{66}Dy^{160}$	85	1.8×10^{-9}	5.8	1.77×10^{-8}	$2+\rightarrow0+$
$_{64}Gd^{154}$	123.2	1.2×10^{-9}	1.42	4.2×10^{-9}	$2+\rightarrow0+$
$_{62}Sm^{152}$	122	1.4×10^{-9}	1.27	4.6×10^{-9}	$2+\rightarrow0+$

tations of Gellman, Griffith, and Stanley,[14] and the partial L-shell values of Rose, Goertzel, and Swift.[15] Conversion in higher shells ($M+N+\cdots$) was taken as $\frac{1}{3}$ of the total L conversion. The total conversion estimate may be systematically high, since screening is neglected in the computations of Gellman, Griffith, and Stanley.[14] A crude estimate based on comparing measured and "theoretical" conversion coefficients[16,17] for Yb^{170} and Er^{166} indicates that on the average, the conversion estimates should not be seriously in error. Estimates of $E2$ radiative lifetimes[2,3] on the single-particle model are known to overestimate lifetimes in the rare-earth region by a large factor (~100). It is interesting to note that $E2$ γ-transition probabilities in even-even nuclei vary in a smooth fashion with neutron number N (or with Z) throughout the region investigated. Figure 4 is essentially a plot of $|1/M|^2$

[14] Gellman, Griffith, and Stanley, Phys. Rev. **85**, 944 (1952).
[15] Rose, Goertzel, and Swift (privately circulated tables).
[16] Graham, Wolfson, and Bell, Can. J. Phys. **30**, 459 (1952).
[17] A. W. Sunyar, Phys. Rev. **93**, 1345 (1954).

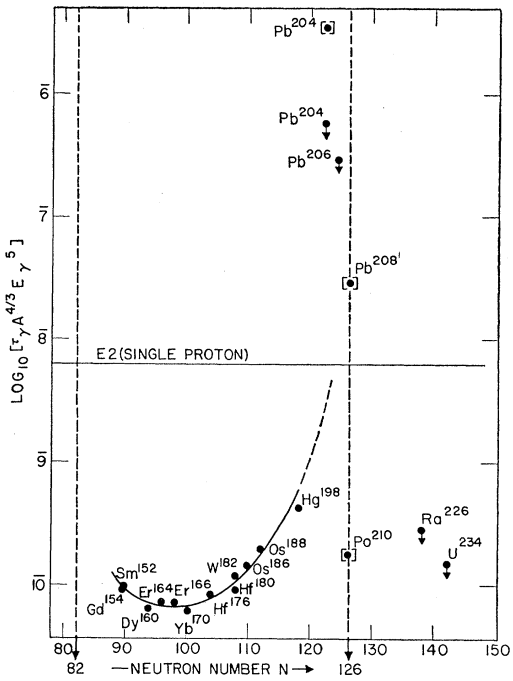

FIG. 4. Comparative lifetimes for $E2$ transitions in even-even nuclei plotted against neutron number N. The theoretical $E2$ line corresponds to unit matrix element on the basis of single particle models. All points except those marked [ ] are $2+\rightarrow0+$ transitions.

(single proton units) *vs* neutron number N. It is seen that maximum matrix elements are reached near $N=98$ and that the matrix elements vary smoothly with N. A marked reduction in radiative transition probability occurs as the doubly magic nucleus Pb^{208} ($Z=82$, $N=126$) is approached.

A summary of information concerning pure $E2$ transitions in odd-A nuclei in the same region of the periodic table is given in Table IV. Information concerning mixed $M1+E2$ transitions in odd-A nuclei is summarized in Table V. An evaluation of the electric quadrupole transition probability for a mixed transition requires knowledge of the relative proportions of $M1$ and $E2$ quanta in the transition. This information is listed in Table V. Figure 5 is a plot showing the variation of $|1/M|^2$ with neutron number N for the $E2$ transitions in odd-A nuclei. Most of the $E2$ transition probabilities in odd-A nuclei exceed the single particle

TABLE IV. Summary of $E2$ γ-ray lifetimes for pure $E2$ transitions in odd-A nuclei.

Nucleus	E(kev)	$T_{\frac{1}{2}}$(sec)	Estimated conversion	τ_γ(sec)
$_{82}Pb^{207}$	570	$<4\times10^{-10}$	~0.021	$<5.8\times10^{-10}$
$_{80}Hg^{199}$	159	2.4×10^{-9}	1.03	7×10^{-9}
$_{80}Hg^{197}$	133	7×10^{-9}	2.15	3.2×10^{-8}
$_{77}Ir^{193}$	73	6.2×10^{-9}	23.3	2.17×10^{-7}
$_{73}Ta^{181}$	133	18.8×10^{-6}	1.4	6.6×10^{-5}
$_{72}Hf^{177}$	112	$<5\times10^{-10}$	2.7	$<2.7\times10^{-9}$

TABLE V. Summary of $E2$ γ-ray lifetimes for mixed $M1+E2$ transitions in odd-A nuclei.

Nucleus	E(kev)	$M1/E2$ γ intensity	Estimated conversion	$T_{\frac{1}{2}}$(sec)	$\tau_\gamma(E2)$ in sec
$_{81}Tl^{203}$	279	1/4[a]	0.20	$\tau_\gamma \cong 10^{-9}$ [b]	1.25×10^{-9}
$_{80}Hg^{199}$	209	$\sim$1/1[c]	$\sim$0.7	$\tau_\gamma = 3.1\times10^{-10}$ [d]	6.2×10^{-10}
$_{79}Au^{197}$	77.4	7/1[e]	5.9	1.9×10^{-9}	1.5×10^{-7}
$_{77}Ir^{191}$	82.3	1.5/1[e]	14	3.85×10^{-9}	2.1×10^{-7}
$_{77}Ir^{191}$	129	5/1[e]	4.4	$<5\times10^{-10}$	$<2.34\times10^{-8}$
$_{73}Ta^{181}$	480	1/1.5[f]	$\sim$0.04	1.2×10^{-8} [g]	3×10^{-8}
$_{73}Ta^{181}$	345	1/1[f]	$\sim$0.1	7.1×10^{-8} [g]	2.2×10^{-7}
$_{73}Ta^{181}$	137	4/1[f]	$\sim$2.3	$<10^{-9}$	$<2.4\times10^{-8}$

[a] S. Thulin and K. Nybö, Arkiv Fysik **7**, 289 (1954); Wapstra, Maeder, Nijgh, and Ornstein, Physica **20**, 169 (1954).
[b] F. R. Metzger and W. B. Todd, Phys. Rev. **95**, 627(A) (1954).
[c] Based on K conversion coefficient measurements of P. M. Sherk and R. D. Hill, Phys. Rev. **83**, 1097 (1951), and K. Siegbahn, reported in *Manne Siegbahn 1886—Three Twelfth 1951* (Almqvist Wiksells Boktrycheri, A.B., Uppsala, 1951), p. 199. Reference e lists this transition as a pure $M1$ transition, based on relative L-shell conversion coefficients.
[d] F. R. Metzger and W. B. Todd, Phys. Rev. **94**, 794(A) (1954).
[e] J. W. Mihelich and A. de Shalit, Phys. Rev. **93**, 135 (1954).
[f] F. K. McGowan, Phys. Rev. **93**, 471 (1954).
[g] Partial half-life based on γ-ray intensities of F. K. McGowan, Phys. Rev. **93**, 163 (1954).

estimates by a considerable factor and do not appear to differ essentially from those for the even-even nuclei. The data for the mixed transitions are subject to an additional uncertainty in that knowledge of the $E2/M1$ gamma-ray mixing ratio is required. Three $E2$ transitions in one nucleus (Ta^{181}) are glaring exceptions to the general trend for $E2$ transition probabilities.

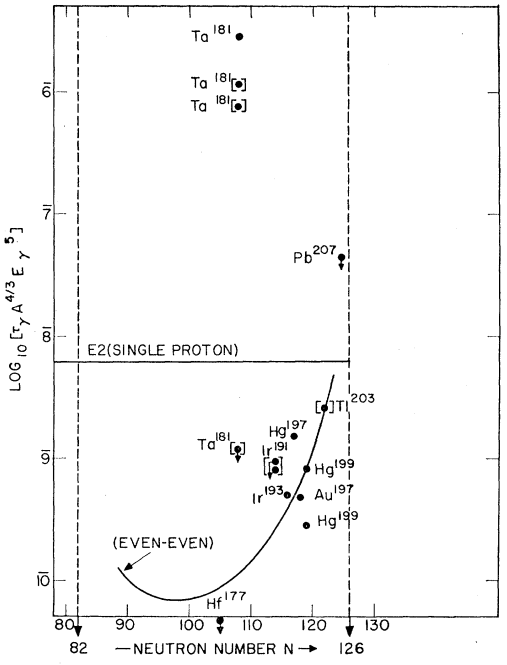

FIG. 5. Comparative lifetimes for $E2$ transitions in odd-A nuclei plotted against neutron number N. The theoretical $E2$ line corresponds to unit matrix element on the basis of single particle models. No statistical weight correction has been made, since initial and final spins are not known with certainty in all cases. Points marked [ ] are mixed $M1+E2$ transitions with the $E2$ transition probability deduced from the $M1/E2$ mixing ratio. The average behavior of the matrix elements for $E2$ transitions in even-even nuclei is shown for purposes of comparison.

In the unified nuclear model of Bohr and Mottelson,[7] the $E2$ radiative transition probability between successive levels in a rotational spectrum gives a measure of the intrinsic quadrupole moment Q_0 of a nuclear state. It is convenient to express the $E2$ radiative lifetime[7] in terms of a distortion parameter β which appears through the dependence of Q_0 on the nuclear shape. For purposes of numerical evaluation we choose the nuclear radius $R_0=1.2\times10^{-13}A^{\frac{1}{3}}$. Then, for $E2$ transitions in *even-even* nuclei between rotational states $I+2\rightarrow I$, we evaluate the γ-ray transition probability as

$$\lambda_\gamma = 2.18\times10^{8}A^{4/3}E^{5}Z^{2}\beta_\tau{}^{2}\frac{(I+1)(I+2)}{(2I+3)(2I+5)}\ \text{sec}^{-1},$$

where A is the mass number, Z is the atomic number, β_τ is the distortion parameter to be evaluated, and E is the transition energy in Mev.

The distortion parameter β may also be evaluated[7] from the magnitude of the energies of rotational states

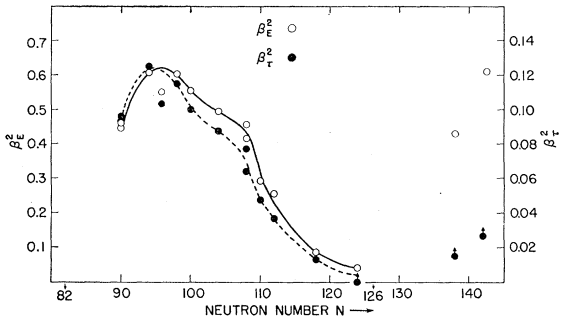

FIG. 6. Distortion parameters $\beta_E{}^2$ and $\beta_\tau{}^2$ for even-even nuclei plotted against neutron number N. Note the different scale for $\beta_E{}^2$ and $\beta_\tau{}^2$.

through the dependence of the moment of inertia on the deformation. (We label β determined from excited state energies as β_E.) Choosing $R_0=1.2\times10^{-13}A^{\frac{1}{3}}$ and evaluating all numerical factors, we find

$$\beta_E{}^2 = 2.43\times10^{5}/A^{5/3}E,$$

where A is the mass number and E is the first excited state energy expressed in kev. Bohr and Mottelson[7] have noted that β_E exceeds β_τ. Ford[18] has pointed out that near $N=82$, the values of β^2 deduced from isotope shift measurements are about four times smaller than those calculated from the energies of the first excited states of even-even nuclei, if one assumes that these are rotational states in the strong-coupling[7] approximation.

Figure 6 exhibits the dependence of $\beta_E{}^2$ and $\beta_\tau{}^2$ on neutron number N for even-even nuclei. Both $\beta_E{}^2$ and $\beta_\tau{}^2$ exhibit qualitatively the same behavior with neutron number, reaching a maximum near $N=95$ and decreasing to low values as the neutron shell closes at

[18] Kenneth W. Ford, Phys. Rev. **95**, 1250 (1954).

$N=126$. Large deformations have again appeared near $N=140$. The ratio $(\beta_E/\beta_\tau)^2$ increases from a value of ~ 4.9 at $N=90$ to a value of $\sim 6.5-7$ for $N=108$ to 118. The exact value of $(\beta_E/\beta_\tau)^2$ depends upon the value chosen for the nuclear radius, since the moment of inertia is proportional to $R_0^2\beta^2$ while Q_0^2 is proportional to $R_0^4\beta^2$. However, any reasonable adjustment of the nuclear radius does not remove the discrepancy. The shoulder on both curves, beginning near $N=100$, may be associated with the filling of $i_{13/2}$ neutron orbits.

The large discrepancy between the absolute values of β_E^2 and β_τ^2 is especially interesting. β_E^2 is essentially a measure of mass deformation while β_τ^2 is a measure of charge deformation *of the quadrupole type*. While quadrupole deformation is expected to be the most important type, a nuclear deformation involving higher multipoles could increase the moment of inertia without contributing to quadrupole transition probabilities. A possible consequence of an appreciable octupole deformation is an enhanced $E3$ transition probability. Such $E3$ transitions have not as yet been experimentally observed in this region of the periodic table. Other possible factors which may contribute to the discrepancy have been discussed by Ford.[18]

Any essential difference between the deformation properties of the neutron structure and the proton structure will lead to different values of β_E^2 and β_τ^2. If such differences exist, they might be best revealed through measurements of the gyromagnetic ratio, since the gyromagnetic ratio of the core depends upon the particular manner in which angular momentum is distributed among the constituents of the core. A breakdown of the assumption of irrotational flow can of course explain the observed large moments of inertia.

We would like to express our appreciation to Dr. M. Goldhaber and Dr. J. Weneser for several interesting discussions, to R. L. Chase and W. Higginbotham for advice in equipment design, and to Dr. D. E. Alburger, Dr. E. L. Church, and Dr. J. W. Mihelich for making certain radioactive sources available to us.

PHYSICAL REVIEW VOLUME 98, NUMBER 3 MAY 1, 1955

Low-Energy Protons from Targets Bombarded by 15-Mev Deuterons*

F. A. ASCHENBRENNER†
Physics Department and Laboratory for Nuclear Science, Massachusetts Institute of Technology, Cambridge, Massachusetts
(Received December 6, 1954)

A particle-selection technique is described which makes it possible to identify readily the reaction particles from deuteron-induced reactions. The results of a study of the low-energy protons from targets bombarded by 15-Mev deuterons is presented. The proton energy spectra from niobium, silver, antimony, tantalum, three lead isotopes, and uranium bombarded with the direct deuteron beam were observed at several angles. In addition, the proton energy spectrum from tantalum was observed at several deuteron beam energies ranging from approximately 10.5 to 15 Mev. The low-energy parts of the proton spectra show what appears to be a Coulomb barrier effect. However, protons are observed several Mev below the Coulomb barrier for protons, indicating that the barrier effect differs from the ordinary Coulomb barrier penetration of protons emerging from a compound nucleus. The behavior of the barrier effect with respect to changes in counter angle, Z (atomic number), and A (mass number) of the targets, and deuteron beam energy was observed.

I. INTRODUCTION

WHEN thin targets are bombarded with deuterons, several types of particles are emitted. Of these, protons and neutrons have been found to be the most abundant. In general, the yield for deuteron-induced reactions is much larger than that of corresponding reactions with other charged particles. For this reason, deuterons are commonly accelerated in cyclotrons for the purpose of radioactive isotope production.

In recent years (d,p) reactions have been subjected to large numbers of experimental and theoretical investigations. In general these investigations have been conducted for two purposes. These are: (1) A study of the properties of the energy levels of the residual nuclei through observations of the proton energy groups; (2) A study of the mechanism of the (d,p) reaction.

Symbolically, the (d,p) reaction can be written:

$$X+d\rightarrow Y+p+Q,$$

where X is the target nucleus; Y is the residual nucleus; and Q is the reaction energy balance, commonly called the Q of the reaction. For a Q greater than -2.23 Mev (where 2.23 Mev is taken to be the binding energy of the deuteron), the residual nucleus is stable against neutron emission and in general, against any heavy-particle emission. For Q less than or equal to -2.23 Mev, sufficient energy has been transferred to the

* Submitted to the Department of Physics, Massachusetts Institute of Technology in partial fulfillment of the requirements for the degree of Doctor of Philosophy. This work has been supported in part by the joint program of the Office of Naval Research and the U. S. Atomic Energy Commission.
† Now at the ANP Department of the General Electric Company, Cincinnati, Ohio.